Ion-counting nanodosimetry: current status and future applications

R. Schulte[1], V. Bashkirov[1], G. Garty [2], S. Shchemelinin[2], I. Orion[2], A. Breskin[2], R. Chechik[2], and B. Grosswendt[3]

1. Dept. of Radiation Medicine, Loma Linda University Medical Center, Loma Linda, CA 92354, USA
2. Dept. Particle Physics, Weizmann Institute of Science, Rehovot, 76100, Israel
3. Physikalisch-Technische Bundesanstalt (PTB), Braunschweig, D-38116, Germany

ABSTRACT

There is a growing interest in the study of interactions of ionizing radiation with condensed matter at the nanometer level. The motivation for this research is the hypothesis that the number of ionizations occurring within short segments of DNA-size subvolumes is a major factor determining the biological effectiveness of ionizing radiation. A novel dosimetry technique, called nanodosimetry, measures the spatial distribution of individual ionizations in an irradiated low-pressure gas model of DNA. The measurement of nanodosimetric event size spectra may enable improved characterization of radiation quality, with applications in proton and charged-particle therapy, radiation protection, and space research. We describe an ion-counting nanodosimeter developed for measuring radiation-induced ionization clusters in small, wall-less low-pressure gas volumes, simulating short DNA segments. It measures individual radiation-induced ions, deposited in 1 Torr propane within a tissue-equivalent cylindrical volume of 2-4 nm diameter and up to 100 nm length. We present ionization cluster size distributions obtained with 13.6 MeV protons, 4.25 MeV alpha particles and 24.8 MeV carbon nuclei in propane; they correspond to a wide LET range of 4-500 keV/micron. We are currently developing plasmid-based assays to characterize the local clustering of DNA damage with biological methods. Systematic comparison of biological and nanodosimetric data will help us to validate biophysical models predicting radiation quality based on nanodosimetric spectra. Possible applications for charged particle radiation therapy planning are discussed.

INTRODUCTION

Nanodosimetry is a natural extension of microdosimetry, developed by H.H. Rossi and his colleagues more than 40 years ago [1], into the nanometer domain. Many of the concepts that were originally developed for microdosimetry apply directly to nanodosimetry. One of these concepts is that of sites, which are geometrically well-defined regions in which the energy absorbed or the number of energy transfers are studied. While experimental microdosimetry, due to technical limitations and prevailing radiobiological thinking at that time, was developed for sites of micrometer dimensions, experimental nanodosimetry focuses on cylindrical sites of nanometer dimensions, simulating short segments of DNA.

A more advanced concept of microdosimetry, *structural microdosimetry*, was first described by Kellerer [2]. It aims at a detailed description of the microscopic pattern of energy transfers in matter and studies the relationship of these patterns with structural features of the sensitive sites in irradiated matter. Over the last 20 years theoretical track structure simulations have attempted to fulfill the goals of structural microdosimetry; however, an experimental technique capable of detailing the full pattern of energy absorption with nanometer resolution has yet to be developed.

The development of experimental nanodosimetry, either based on the concept of nanometer sites or, eventually, resolving the pattern of energy deposition with nanometer resolution, is driven by the increasing acceptance of the concept that DNA clustered damage in regions having dimensions of the order of 10 nm plays a major role in the biological effectiveness of ionizing radiation [3, 4].

In recent years, we have developed an experimental nanodosimetric technique that measures the number of charges deposited in a small volume of low-density gas simulating a DNA site [5-7]. Nanometer spatial resolution is possible by collecting positive ions [8] rather than electrons [9] from the irradiated sensitive volume, then extracting them by an electric field into vacuum where they are accelerated and recorded by an ion counter. The size of the sensitive volume is determined by the gas pressure, the electric field geometry, and the diameter of the extraction aperture. It was shown that sensitive volume dimensions ranging from less than 1 nm to 4 nm in diameter and up to 100 nm in length can be achieved with this technique.

In this paper we describe the details of the ion-counting nanodosimetric technique, report on results of performance studies, and discuss future applications of nanodosimetry.

EXPERIMENTAL NANODOSIMETRY

Nanodosimetric site concept

The original site concept of microdosimetry was concerned with the energy deposition or the number of energy transfers in volumes of specified microscopic dimensions. The amount of energy deposited is related to the rate of energy loss by the charged particles that are responsible for the energy deposition; in other words, the linear energy transfer (LET) of the primary particles. However, since LET can only characterize the mean energy deposited in a given volume, it contains no information about the stochastic distribution of energy deposition events. On the other hand, the latter is believed to be of great importance for the biological effectiveness of ionizing radiation.

In nanodosimetry, the relevant sites are cylinders of 2-4 nm diameter and 16 nm length, corresponding to short segments of DNA of about 50 base pairs and the surrounding water layer. In a previous publication, it was shown that the statistical distribution of the number of ionizations in 2 nm by 16 nm cylindrical sites, calculated by Monte Carlo track structure simulation of charged particle tracks in water vapor, was significantly related to the RBE of protons and helium ions [10].

In order to simulate such conditions realistically, one has to create a relatively large ionization volume in which a much smaller, ideally wall-less, sensitive site is embedded. Ions produced within the core of the sensitive volume should be collected with high efficiency, simulating the direct ionization of the DNA itself. Ions produced in the adjacent volume should be collected with an efficiency that falls off in a distance-dependent manner simulating the indirect radiation effect on DNA in which hydroxyl radicals or other reactive species of water radiolysis react with DNA.

The ion-counting nanodosimeter

Fig. 1 shows a detailed view of the ion-counting nanodosimeter, currently in operation at the Weizmann Institute of Science and at Loma Linda University. The nanodosimeter and its performance are described in detail elsewhere [11]. The accelerator-generated primary particle beam traverses a low-pressure gas ionization volume (IV) and reaches a trigger detector (not shown). Ions induced in the ionization volume are extracted into an evacuated detection volume (DV) and registered by an ion counter. For each primary particle event, a dedicated data acquisition system (DAQ) registers both the number and arrival time of the ions with respect to the trigger. In addition, the DAQ may record energy and position of the primary particle.

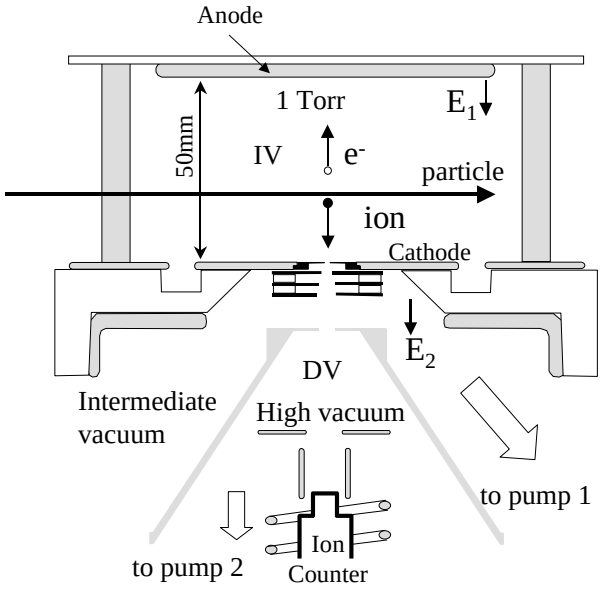

Fig. 1. Schematic diagram of the ion-counting nanodosimeter; for details see text.

In the present setup, the ionization volume is filled with propane at a density of $2.4 \cdot 10^{-6}$ g/cm^3. Under these conditions, a mean free path length of 1 mm in gas corresponds to 2.4 nm in condensed matter. Via the electric fields E_1 and E_2, ions are drifted and extracted through a 1mm aperture into the intermediate vacuum region (10^{-3} Torr) and are then accelerated into the ion detection volume ($3 \cdot 10^{-5}$ Torr). The five orders of magnitude pressure difference between the ionization volume and the detection volume is achieved by a double-differential pumping system, consisting of two turbomolecular pumps.

The size and shape of the wall-less sensitive volume (SV) embedded into the ionization volume are determined by the transport of ions in the gas and their extraction efficiency through the aperture. Varying the gas density, the aperture diameter as well as the electric field E_1 above and E_2 below the ion extraction aperture one can tune the sensitive volume size and shape.

The SV may be represented by a map of iso-efficiency contours, corresponding to equal ion extraction efficiencies (Fig. 2). These maps can be calculated based on the simulated electric field geometry and on measured transport parameters of propane ions [7]. The sensitive volume diameter is broader than that of the aperture due to penetration of the electric field E_2 from the acceleration electrodes through the aperture, imposing some additional focusing.

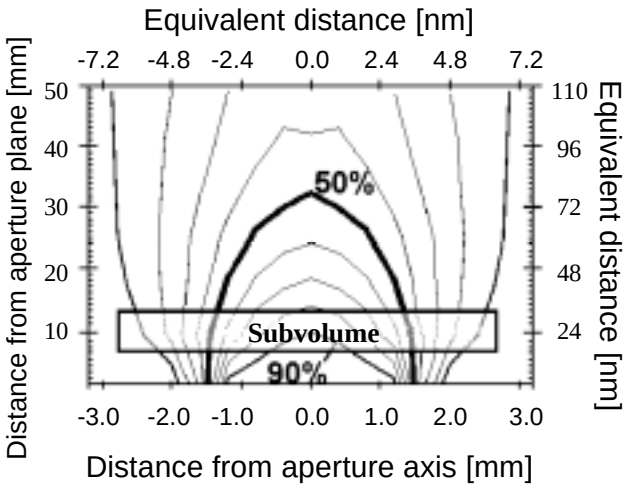

Fig. 2 Monte Carlo-simulated maps of the ion extraction efficiency, defining the wall-less sensitive volume. Each contour line represents a change of 10% in the ion collection efficiency (the thick line is 50%). The bottom and left scales are real distances in gas, while the top and right scales provide the tissue-equivalent distances in nanometer. Note that the vertical scale is compressed by factor ~15 compared to the horizontal one.

From a given SV one may select a subvolume of defined length based on time cuts applied to the ion arrival time to the ion counter. One can thus define a cylinder-like SV of approximately 4-6 nm diameter and 16 nm length, which is characterized by an ion collection efficiency profile that simulates the desired nanodosimetric site.

The nanodosimeter contains a gold-plated ^{241}Am alpha source for internal calibration and monitoring of system performance. The source has an average energy of 4.25 MeV with a width of 0.3 MeV (FWHM), corresponding to an average LET of 107 keV/micron in water. The collimated alpha particles are triggered by a PIN diode, located across from the SV region. This results in a beam with 1 mm diameter (FWHM) crossing the sensitive volume at its vertical axis at a distance of 15 mm above the ion extraction aperture and perpendicular to the accelerator beam axis. During external beam operation, the alpha particle beam can be turned off using a shutter. The accelerated particle beam crosses the sensitive volume at its vertical axis at 15 mm above the extraction aperture. Appropriate collimators placed at the nanodosimeter entrance and the trigger detector define the beam diameter.

Within the evacuated detection volume, ions are accelerated to about 8keV onto the ion counter (a discrete dynode electron multiplier, EM, SGE model AF180HIG) whereby they are individually detected and counted.

PERFORMANCE STUDIES

Experimental setup

A series of performance studies with the goal to characterize and optimize the ion-counting operation of the nanodosimeter was performed at the Weizmann Institute of Science, where the nanodosimeter has been mounted at the UD14 Pelletron accelerator. For the performance studies, accelerated protons and carbon ions, as well as the internal alpha particles, were used.

Fig. 3 shows the experimental setup: the external ion beam from the Pelletron traverses a thin scattering foil and a system of three 1-mm diameter apertures producing a low intensity beam, which passes through the ND at different locations with respect to the sensitive volume. The collimated ion beam enters and exits the ND via a thin (2.5 μm) Mylar window of 15 mm diameter. The beam localization and triggering system consists of a 2D-position sensitive multiwire proportional chamber (MWPC), followed by a 5 mm thick plastic scintillation detector, which is coupled to a photomultiplier tube (PMT) and collimated to 1 mm diameter [11].

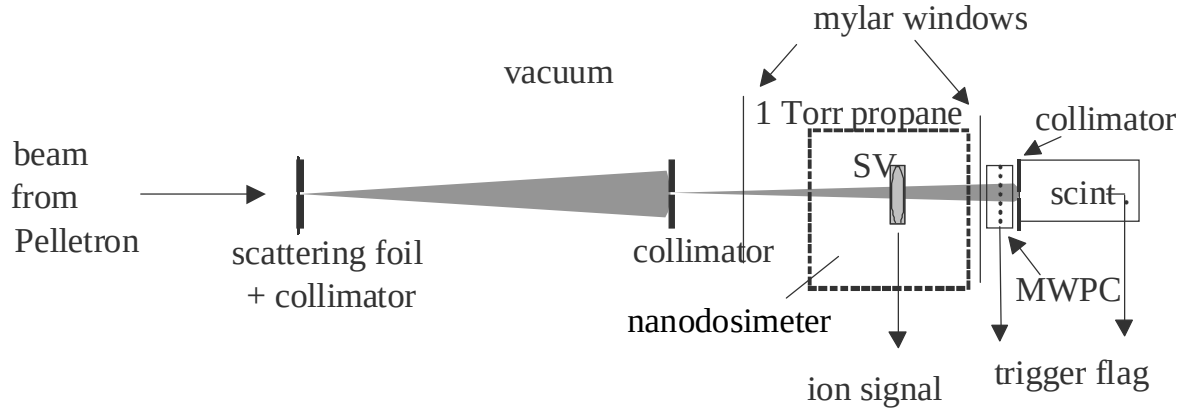

Fig. 3. A schematic diagram of the beam line setup for performance studies at the Weizmann Institute of science; for details see text.

The trigger and the offline analysis permit for an efficient pileup rejection [11]. All elements along the beam line were optically aligned ensuring that the beam axis passed the vertical axis of the SV 15 mm above the ion extraction aperture with an accuracy of better than ± 0.2 mm.

Cluster size distributions of particles with different LETs

Fig. 4 shows measured ion cluster size spectra, recorded with the nanodosimeter, of 13.6 MeV protons (LET of 3.8 keV/micron in water), 4.25 MeV alpha particles (LET of 107 keV/micron in water) and 24.8 MeV carbon ions (LET of 500 keV/micron in water). All beams were identical in diameter (1 mm, FWHM) and crossed the SV at the same distance from the ion extraction aperture (15 mm). The electrical field conditions were chosen to generate a SV with a 50% efficiency contour of maximal diameter equivalent to 4.2 nm and length equivalent to 100 nm in unit density medium (see Fig. 2). No time selection was applied. The spectra in Fig. 4 are displayed as absolute frequencies per incident particle. As expected, the average cluster size increases according to the increase in LET.

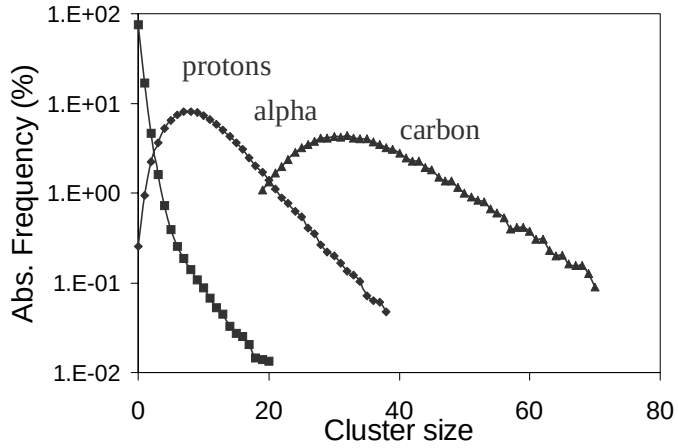

Fig. 4. Nanodosimetric cluster size distributions for 13.6 MeV, 4.25 MeV alpha particles and 24.8 MeV carbon ions. All spectra were obtained under equivalent experimental conditions.

One should note that these spectra, recorded with a pencil bean for performance studies, are biologically not very relevant. What matters for radiobiology is a situation, where charged particles pass at random distances from the site and most of the energy is deposited inside the site by secondary charged particles, mostly electrons. Measurements of such broad beam spectra are underway.

APPLICATIONS OF NANODOSIMETRY

General strategy

A broad goal of both experimental nanodosimetry and theoretical track structure simulation is to relate some of the principal features of microscopic energy deposition in nanometer sites to the biological features produced by ionizing radiation, in particular the complexity of DNA damage. One may argue that track structure simulations of DNA damage are more accurate in this respect since they take into account condensed phase effects, energy transfers other than ionizations, and the complex structural folding of the DNA molecule in chromatin. On the other hand, experimental nanodosimetry, even with its simplifications, is more versatile in situations where mixed and complex radiation fields, radiations of unknown composition, or radiation with time-dependent quality are studied. Examples include therapeutic radiation and space radiation.

The development of nanodosimetry for applications in radiation therapy and radiation protection involves several steps (Fig. 5). Nanodosimetry provides ionization event spectra in DNA sites exposed to a broad beam of the radiation of interest. A biophysical model is devised that transforms these spectra into DNA damage spectra, i.e., the frequency distributions of the number of DNA lesions per DNA damage cluster. The biophysical model is validated using a radiation experiment with DNA, which measures biological parameters that are uniquely related to the level of DNA lesion clustering. Alternative biophysical models or different sets of model parameters for the same model may then be tested to see how well they can reproduce the experimentally

measured biological parameter. Using the DNA damage spectra, a biological weighting factor, which may be used in various applications, is defined.

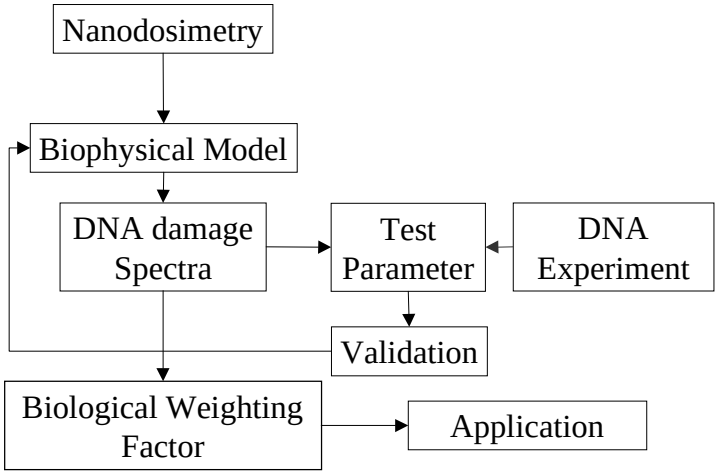

Fig. 5. Steps in the development of nanodosimetry for applications in radiation therapy and radiation protection.

Ionization clusters and complex DNA damage

The major products in irradiated DNA, produced by direct or indirect effects, are various base oxidations and strand breaks. Track structure simulations [12, 13] have predicted clustering of these lesions over distances of 10 nm or less and, more recently, experimental evidence has supported this prediction [14, 15].

The assumption that the highly non-homogenous structure of charged particle tracks is directly related to the local clustering of DNA lesion, which are predominantly caused by direct ionization of DNA or, indirectly, by ionization of nearby water molecules, is straightforward. We have begun to investigate the use of a plasmid model system to define experimental parameters, which correlate with the level of clustering in complex DNA lesions. The advantage of such a biological model system is that it can be prepared and studied in a well-defined chemical environment that simulates the OH radical scavenging capacity of a cell without interference from cellular repair processes.

In the most basic form, plasmid assays only detect and quantify double strand breaks, which form the linear band after standard agarose gel electrophoresis [16]. Other forms of complex damage, in which strand breaks are combined with base damages, may be distinguished by incubating the irradiated DNA with purified glycosylases or endonucleases [15, 17]. As the average cluster size will increase with increasing LET, it can be shown, based on modeling studies, that the ratio of the frequency of all complex lesions to that of double strand breaks decreases from a value of approximately 12 for low-LET irradiation to close to one for high-LET irradiation (Fig. 6).

To verify this experimentally, we studied the ratio of the frequency of all double-stranded plasmid lesions, and the frequency of double strand breaks for low-LET gamma rays, and high-LET alpha particles. It was found that this ratio followed the expected LET dependence: it had a value of 10-15 for low-LET gamma irradiation and a value of 2-4 for high-LET irradiation [unpublished results].

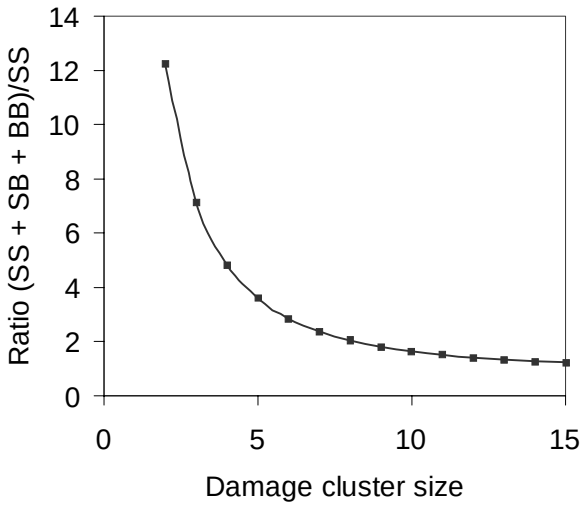

Fig. 6. Modeling results showing the ratio of the frequency of double strand breaks in plasmids to that of all other complex double-stranded DNA lesions as a function of damage cluster size.

Complex DNA damage and cellular repair

Track structure model calculations as well as experimental nanodosimetric spectra predict that the majority of DNA damages consist only of one lesion such as a base damage or a single strand break, while the frequency of more complex lesions decreases by orders of magnitude with increasing cluster size.

Enzymatic processes, using the opposing strand as a template, easily repair the single damages. Repair of low-LET double strand breaks, mostly consisting of two breaks separated by variable number of bases (up to 30), is also common in cells and most likely represents independent repair of its constituent single strand breaks. Base excision repair, which is very effective for single base damages, forms additional strand breaks during the repair process, which are subsequently annealed.

As the complexity of the damage increases its reparability decreases. Fig. 7 shows the (hypothetical) relationship between the probability of repair as a function of lesion cluster size. One may assume that different cell types, or cells irradiated under different conditions or during different phases of the cell cycle, differ in their capability to repair smaller DNA damage clusters, while the repair of large clusters (number of lesions > 5) is uniformly impossible. The repair capacity for smaller clusters, which are the most frequent form of damage, may also depend on the dose level and the dose rate, explaining the non-linear shape of most low-LET cell survival curves.

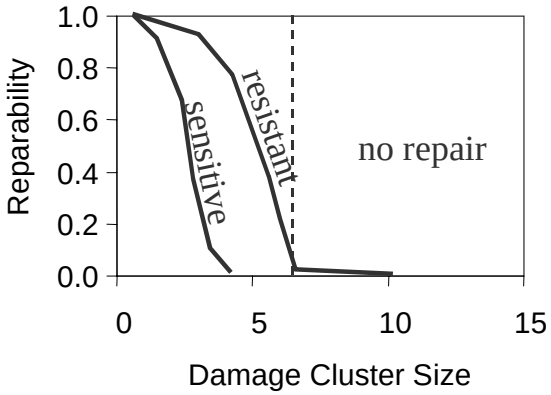

Fig. 7. Hypothetical relationship between the probability of repair of complex DNA damage as a function of damage cluster size.

Biological weighting factor

Based on what has been discussed so far, it is reasonable to assume that the most relevant biological damage consists of clusters containing 6-10 individual DNA lesions since they are uniformly irreparable. The majority of these damages will appear as overt double strand breaks. A biological weighting factor (*BWF*) may be defined as the following frequency ratio:

$$BWF = \frac{\sum_{j=6}^{10} f(j)}{\sum_{j=6}^{10} f_{ref}(j)}$$

where $f(j)$ and $f_{ref}(j)$ are the DNA cluster size frequency distributions for the experimental and reference radiation, respectively. These are defined on a unit-fluence basis, e.g., per incident particle. The advantages of this definition are obvious: because DNA clusters are single-track events the *BWF* is fluence (or dose) independent; the *BWF* characterizes the production of biologically relevant damage, which can be expected to be produced with similar yields independent of the biological system.

Biological weighting factor and radiotherapy planning

Because of their favorable depth-dose characteristics, high-energy protons and heavier ions are increasingly being used for radiation therapy [18, 19]. For ion beam applications, some assumptions about the RBE with respect to low-LET-reference radiation are usually made. While for high-LET beams such as carbon, measurable changes of the RBE throughout the spread-out Bragg peak (SOPB) are generally taken into account [20], for protons, where the RBE changes are much more subtle, a constant generic RBE of 1.1 is usually assumed [21]. On the other hand, changes of biological quality with penetration depth have also been detected for therapeutic proton beams with cell survival assays and microdosimetry measurements [22].

Since proton treatment planning systems display only physical dose but not biologically effective dose, the treatment planner is not alerted to situations where critical tissues may be exposed to doses of higher biological effectiveness, as is expected in the distal SOBP region. Even if some assumptions about the depth dependence of RBE are made, there are inherent weaknesses in the RBE concept. One of the major problems with RBE is that it represents a ratio of doses for a given iso-effect level rather than a ratio of biological effectiveness for different types of radiation. Determinations of RBE also depend on the choice of the biological endpoint and the selection of physical beam parameters. Non-linear dose response relationships further complicate the RBE issue by making RBE dependent on dose and effect level [23].

The use of a *BWF* based on nanodosimetric measurements in a mixed therapeutic proton or ion beam is an attractive alternative to the clinical RBE concept. Because the *BWF* is independent of dose it can be treated as a dose-modifying factor, which means that the ratio of doses for equal levels of complex DNA damage is constant for two radiations of different qualities. When using the *BWF* in treatment planning, the treatment planner, in addition to the physical dose distribution, would also evaluate a biologically weighted dose distribution, which is obtained by multiplying physical dose with the depth-dependent *BWF*. The resulting dose distribution more accurately reflects the production of irreparable DNA damage. These biologically weighted dose distributions can then used to develop an optimal treatment plan, which maximizes the biological dose given to the tumor and minimizes the biological dose in critical normal tissues.

CONCLUSIONS

Nanodosimetry is a promising new technique to measure the stochastic pattern of radiation-induced ionizations at the molecular level. An ion-counting nanodosimeter has been developed, and performance studies using a wide range of particles and LETs have been performed. Correlation of nanodosimetric event size spectra with spectra of DNA lesion complexity may pave new ways to standardize the biological characterization of ionizing radiation and to define biological weighting factors for radiation therapy planning and for radiation protection involving mixed radiations with a high-LET component. This may eventually help to overcome problems inherent in the clinical RBE concept and the concept of radiation quality factors currently used in radiation protection.

ACKNOWLEDGEMENTS

The authors would like to thank Prof. M. Hass, Dr. O. Heber and Y. Shachar for their assistance with the accelerator experiments, Mr. M. Klin for his technical assistance, and Dr. J. Milligan for useful discussions of the biological aspects of nanodosimetry. S. Shchemelinin is supported by the state of Israel, the Ministry of Absorption and the Center for Absorption of Scientists. A. Breskin is the W. P. Reuther Professor of Research in the peaceful uses of Atomic Energy.

This work was partially supported by the National Medical Technology Testbed Inc. (NMTB) under the U.S. Department of the Army Medical Research Acquisition Activity, Cooperative Agreement Number DAMD17-97—2-7016 and by the MINERVA Foundation. The views and conclusions contained in this report are those of the authors and do not necessarily reflect the position or the policy of the U.S. Army or NMTB.

REFERENCES

[1] Rossi, H.H., Specification of radiation quality, *Rad. Res.* 10: 522-531, (1959)

[2] Kellerer, A.M., Chmelevsky, D., Concepts of microdosimetry. II. Probability distributions of the microscopic variables, *Radiat. Environ. Biophys.* 12: 205-216, (1975)

[3] Prise, K.M., Pinto, M., Newman, H.C., Michael, B.D., A review of studies of ionizing radiation-induced double-strand break clustering, *Radiat. Res.* 156: 572-576, (2001)

[4] Ward, J.F., The complexity of DNA damage – relevance to biological consequences, Int. J. Radiat. Biol. 66: 427-432, (1994)

[5] Shchemelinin, S., Breskin, A., Chechik, R., Pansky, A., Colautti, P., A nanodosimeter based on single ion counting, In: *Microdosimetry - An interdisciplinary approach*, Eds. Goodhead, D., O'Neel, P., and Menzel, H., The Royal Society of Chemistry, Cambridge, pp 375-378, (1997)

[6] Shchemelinin, S., Breskin, A., Chechik, R., Pansky, A., Colautti, P., Conte, V., De Nardo, L., Tornielli, G., Ionization measurements in small gas samples by single ion counting, *Nucl. Instr. Meth. A*368: 859-861, (1996)

[7] Shchemelinin, S., Breskin, A., Chechik, R., Colautti, P., Schulte, R.W., First ionization cluster measurements on the DNA scale in a wall-less sensitive volume, *Radiat. Prot. Dosim*. 82: 43-50, (1999)

[8] Chmelewski, D., Parmentier, N., Le Grand, J., Dispositif experimental en vue d'etudes dosimetriques au niveau du nanometre. In: *Proceedings of the fourth symposium on microdosimetry*, EUR 5122 d-e-f, CEC, Luxemburg, 1973, p.869

[9] Breskin, A., Chechik, R., Colautti, P., Conte, V., Pansky, A., Schchemelinin, S., Talpo, G., Tornielli, G., A single-electron counter for nanodosimetry. *Radiat. Prot. Dosim.* 61: 199-204, (1995)

[10] Schulte, R., Bashkirov, V., Shchemelinin, S., Garty, G., Chechik, R., Breskin, A., Modeling of radiation action based on nanodosimetric event spectra, *Physica Medica Vol. XVII*: 177-180, (2001)

[11] Garty, G., Shchemelinin, S., Breskin, A., Chechik, R., Assaf, G., Orion, I., Bashkirov, V., Schulte, R., Grosswendt, B., The performance of a novel ion-counting nanodosimeter, Submitted to *Nucl. Instr. & Meth A.*

[12] Nikjoo, H., O'Neill, P., Terrissol, M., Goodhead, D.T., Quantitative modelling of DNA damage using Monte Carlo track structure, *Radiat. Environ. Biophys*. 38: 31-38, (1999)

[13] Nikjoo, H., O'Neill, P., Wilson, W.E., Goodhead, D.T., Computational approach for determining the spectrum of DNA damage induced by ionizing radiation, *Radiat. Res.* 156: 577-583, (2001)

[14] Sutherland, B.M., Bennett, P.V., Sidorkina, O., Laval, J., Clustered damages and total lesions induced in DNA by ionizing radiation: oxidized bases and strand breaks, *Biochemistry* 39: 8026-8031, (2000)

[15] Milligan, J.R., Aguilera, J.A., Paglinawan, R.A., Ward, J.F., Limoli, C.L., DNA strand break yields after post-high LET irradiation incubation with endonuclease-III and evidence for hydroxyl radical clustering, *Int. J. Radiat. Biol.* 77: 155-164, (2001)

[16] Shao, C., Saito, M., Yu, Z., Formation of single- and double-strand breaks of pBR322 plasmid irradiated in the presence of scavengers, *Radiat. Environ. Biophys*. 38: 105-109, (1999)

[17] Milligan, J.R., Aguilera, J.A., Nguyen, T.T., Paglinawan, R.A., Ward, J.F., DNA strand-break yields after post-irradiation incubation with base excision repair endonucleases implicate hydroxyl radical pairs in double-strand break formation, *Int. J. Radiat. Biol*. 76: 1475-1483, (2000)

[18] Loeffler, J.S., Smith, A.R., Suit, H.D., The potential role of proton beams in radiation oncology, *Semin. Oncol*. 24: 686-695, (1997)

[19] Orecchia, R., Zurlo, A., Loasses, A., Krengli, M., Tosi, G., Zurrida, S., Zucali, P., Veronesi, U., Particle beam therapy (hadrontherapy): basis for interest and clinical experience, *Eur. J. Cancer* 34: 459-468, (1998)

[20] Kraft, G., Radiotherapy with heavy ions: radiobiology, clinical indications and experience at GSI, Darmstadt, *Tumori* 84: 200-204, (1998)

[21] Gerweck, L.E., Kozin, S.V., Relative biological effectiveness of proton beams in clinical therapy, *Radiother. Oncol*. 50: 135-142, (1999)

[22] Robertson, J.B., Eaddy, J..M., Archambeau,, J.O., Coutrakon, G.B., Miller, D.W., Moyers, M..F., Siebers, J.V., Slater, J.M., Dicello, J.F., Relative biological effectiveness and microdosimetry of a mixed energy field of protons up to 200 MeV, *Adv. Space Res*. 14: 271-275, (1994)

[23] Jones, B., Dale, R.G., Estimation of optimum dose per fraction for high LET radiations: implications for proton radiotherapy, *Int. J. Radiat. Oncol. Biol. Phys*. 48: 1549-1557, (2000)